Available online at www.sciencedirect.com

ScienceDirect

www.elsevier.com/locate/matchar

Evolution of microstructural defects with strain effects in germanium nanocrystals synthesized at different annealing temperatures

Minghuan Zhang[a,b], Rongsheng Cai[a,b], Yujuan Zhang[a,b], Chao Wang[a,b], Yiqian Wang[a,c,*], Guy G. Ross[d], David Barba[d]

[a]The Cultivation Base for State Key Laboratory, Qingdao University, No. 308, Ningxia Road, Qingdao 266071, PR China
[b]College of Chemistry and Chemical Engineering, Qingdao University, No. 308, Ningxia Road, Qingdao 266071, PR China
[c]College of Physics Science, Qingdao University, No. 308, Ningxia Road, Qingdao 266071, PR China
[d]INRS-EMT, 1650 Boulevard Lionel-Boulet, Varennes, Quebec J3X 1S2, Canada

ARTICLE DATA

Article history:
Received 18 November 2013
Received in revised form
14 March 2014
Accepted 15 March 2014

Keywords:
Ge nanocrystals
Evolution of defects
HRTEM
Stress

ABSTRACT

Ge nanocrystals (Ge-ncs) were produced by implantation of $^{74}Ge^{+}$ into a SiO_2 film on (100) Si, followed by high-temperature annealing from 700 °C to 1100 °C. Transmission electron microscopy (TEM) studies show that the average size of Ge-ncs increases with the annealing temperature. High-resolution TEM (HRTEM) investigations reveal the presence of planar and linear defects in the formed Ge-ncs, whose relative concentrations are determined at each annealing temperature. The relative concentration of planar defects is almost independent of the annealing temperature up to 1000 °C. However, from 1000 °C to 1100 °C, its concentration decreases dramatically. For the linear defects, their concentration varies considerably with the annealing temperatures. In addition, by measuring the interplanar spacing of Ge-ncs from the HRTEM images, a strong correlation is found between the dislocation percentage and the stress field intensity. Our results provide fundamental insights regarding both the presence of microstructural defects and the origin of the residual stress field within Ge-ncs, which can shed light on the fabrication of Ge-ncs with quantified crystallinity and appropriate size for the advanced Ge-nc devices.
© 2014 Elsevier Inc. All rights reserved.

1. Introduction

In the past two decades, much effort has been devoted to the study of germanium nanocrystals (Ge-ncs) due to their wide range of applications in new integrated optoelectronic devices and highly-efficient solar cells [1,2]. Compared with silicon nanocrystals, Ge-ncs exhibit strong visible photoluminescence and electroluminescence, which are suitable for fabrication of light-emitting devices [3–6]. The hole and electron mobilities of bulk Ge are 4.2 and 2.6 times higher than those of Si [7], so that the nanostructured germanium is very promising for the development of high-speed devices. Also, the weak energy bandgap of Ge (0.66 eV) can improve the quantum confinement effects inside Ge-ncs for promoting multiple exciton generation in third generation solar cells [8].

In recent years, ion implantation has been extensively employed to produce Ge-ncs with well-controlled depth and size distribution by adjusting the implantation and annealing

* *Corresponding author at:* The Cultivation Base for State Key Laboratory, Qingdao University, No. 308, Ningxia Road, Qingdao 266071, PR China. Tel./fax: +86 532 83780318.
E-mail address: yqwang@qdu.edu.cn (Y. Wang).

http://dx.doi.org/10.1016/j.matchar.2014.03.010
1044-5803/© 2014 Elsevier Inc. All rights reserved.

conditions [2,9,10]. Until now, a lot of studies have focused on the morphology, size effect and spatial distribution of Ge-ncs [9,11–14]. However, during the formation of Ge-ncs, specific defects can be produced within the nanocrystallites and thus affect their physical properties [15]. The Ge-ncs are also subject to complex stress effects, whose intensity may be related to both the nature and the concentration of their internal defects. The stress in Ge-ncs is generally associated with two different mechanisms: the first one originates from a local lattice mismatch between Ge crystal planes of different orientations, and the second one is related to volume expansion during the annealing process. To our knowledge, the evolution of microstructural defects, as well as their connection with the stress relaxation process as a function of the annealing temperatures has never been explored nor demonstrated.

In this paper, Ge-ncs embedded in the amorphous SiO_2 matrix were fabricated using ion implantation, followed by thermal annealing. The evolution of both Ge-nc dimensions and microstructural defects inside Ge-ncs has been investigated as a function of annealing temperatures using high-resolution transmission electron microscope (HRTEM) imaging. Two kinds of defects, namely planar (twins and stacking faults) and linear (dislocations) defects, are identified and quantified, showing two distinct evolutions. The variations of both dislocation concentration and the interplanar spacing of Ge-ncs give evidence of strong correlations between the formation of dislocations and the stress field, whose formation mechanisms and origins are discussed.

2. Experimental

$^{74}Ge^+$ ions were implanted into a SiO_2 film grown on (100) Si at a fluence of 8×10^{16} cm^{-2}, with an ion energy of 70 keV, using an IBS/IMC 200 commercial implanter. This apparatus consists of a plasma source, a magnet mass separator, an accelerator line and a target chamber. Fig. 1 presents a schematic diagram for the process of ion implantation. Firstly, ions are generated by the plasma source and provided with an initial velocity after the first acceleration. Then, $^{74}Ge^+$ ion isotopes are isolated in the magnet mass separator and are electrostatically accelerated to the desired energy in the accelerator line. Eventually, impinging ions are implanted into the silicon oxide sample in the target chamber. The samples were then separately annealed under ultrahigh purity N_2 atmosphere for 1 h at annealing temperatures of 700 °C, 800 °C, 850 °C, 900 °C, 1000 °C and 1100 °C, respectively. To avoid any accidental contamination by the annealing ambient, the gas flux was filtered using an additional nitrogen purifier.

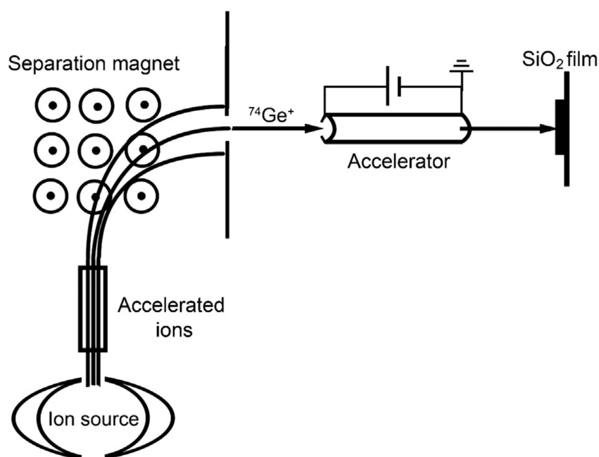

Fig. 1 – The schematic diagram for the process of ion implantation.

The cross-sectional specimens ([011] zone axis for Si substrate) for transmission electron microscopy (TEM) observations were prepared by conventional techniques of mechanical polishing and ion thinning. Selected-area electron diffraction (SAED), bright field (BF) and HRTEM were carried out using a JEOL JEM2100F TEM operating at 200 kV.

3. Results and Discussion

Typical BF TEM images are presented in Fig. 2(a)–(f) for samples annealed at 700 °C, 800 °C, 850 °C, 900 °C, 1000 °C and 1100 °C, respectively. In order to facilitate their comparison as a function of the annealing temperature, all these images were recorded at the same magnification. The BF TEM images were obtained with Si substrates oriented along the [011] zone axis. In Fig. 2, Ge-ncs are observed in the upper region of the SiO_2 film, up to a depth of 65 ± 5 nm in all studied samples. Such a value is consistent with the maximum ion path of 70 keV Ge^+ implanted into a fused silica target, calculated using the SRIM computer code [16]. The average sizes of Ge-ncs are determined from a precise analysis of TEM images and summarized in Table 1. These measurements are plotted in Fig. 3, showing that the size of the Ge-ncs observed in different samples increases with the annealing temperatures, from 5.95 nm at 700 °C to 28.15 nm at 1100 °C. Such an increase of the Ge-nc dimensions can be associated with the coalescence of small nanocrystals, according to a mechanism described in previous reports [10,17]. It is also consistent with the general trend observed by scanning electron microscopy (SEM), for Ge-ncs synthesized at different annealing temperatures in fused silica [2].

Extensive HRTEM analysis reveals two different kinds of microstructural defects inside Ge-ncs, namely, planar defects and linear defects. The relative concentrations of planar and linear defects are presented in Table 2 for each studied sample. Furthermore, the changing trends of different defects are clearly shown in Fig. 4. As shown in Fig. 4(a), the relative concentration of planar defects, especially twinning and stacking faults, is almost independent of the annealing temperature up to 1000 °C. However, from 1000 °C to 1100 °C, its concentration decreases dramatically. For the linear defects, i.e. dislocations, their concentration varies considerably with the annealing temperatures, as shown in Fig. 4(b). Fewer dislocations are observed in the Ge-ncs with an average size smaller than 6 nm annealed at 700 °C. According to some literature [18,19], as the grain size or feature size is reduced, there is a critical size below which the defect content can be virtually reduced to zero. For annealing temperatures increasing up to 900 °C the dislocation percentage increases up to ~26%. It then decreases to ~20% for the annealing at 1000 °C and drastically increases up to ~35% for the annealing at 1100 °C.

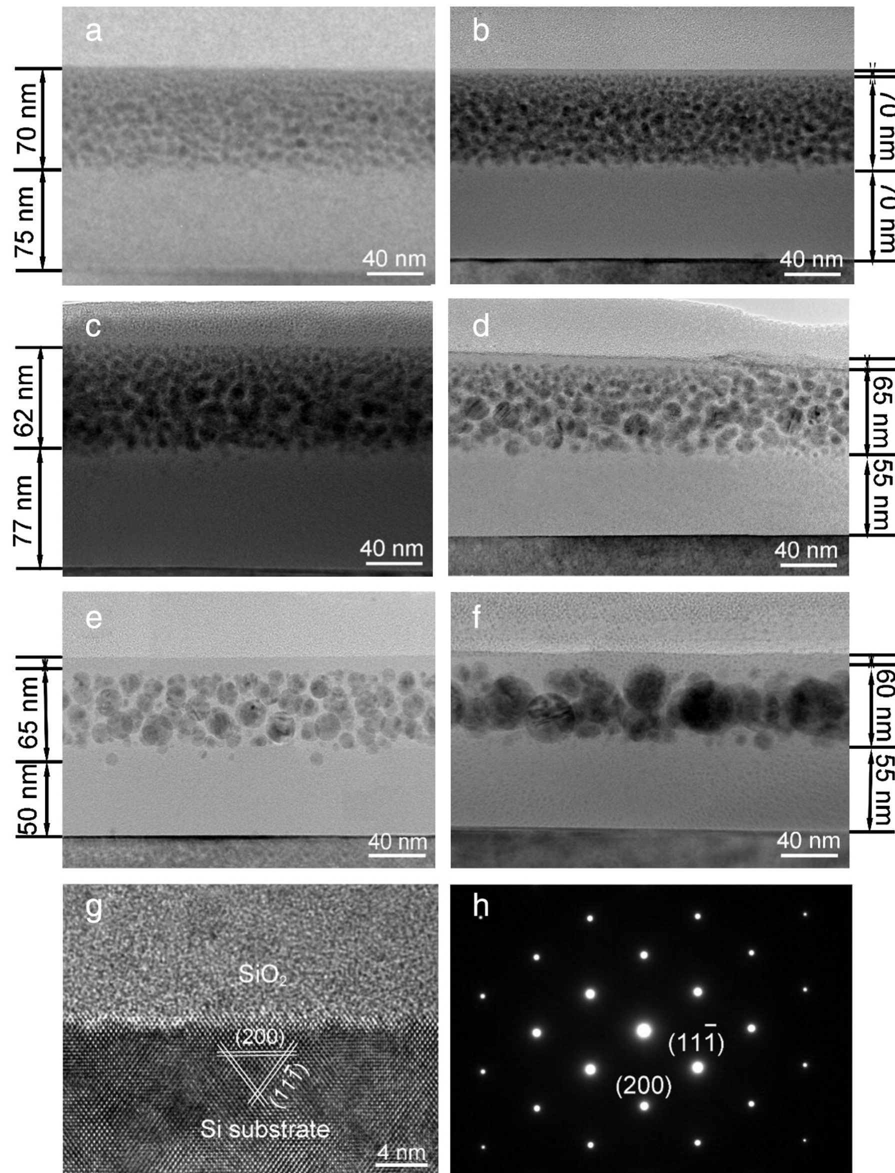

Fig. 2 – Typical BF images showing the spatial distribution of Ge ncs formed at different annealing temperatures: (a)700 °C; (b)800 °C; (c)850 °C; (d)900 °C; (e)1000 °C; (f)1100 °C; (g) HRTEM image taken from the interface region of SiO_2/Si; (h) SAED pattern taken from the Si substrate.

Fig. 5 shows typical HRTEM images of Ge-ncs synthesized at 700 °C. Planar defects, especially twins, are dominant and generally observed in the bigger nanoparticles. However, linear defects are rarely observed at this annealing temperature. As shown in Fig. 5(a), two nanoparticles are about to combine together. Their crystal planes tend to gradually align at the interface. The right particle is composed of crystals with different orientations, which results from the coalescence of small Ge-ncs at the beginning of the annealing process. Such a mechanism is known to significantly reduce the energy of the whole system, because the surface area of coalesced nanoparticles is lower than that of all isolated nanoparticles. Fig. 5(b) shows a combination of three Ge-ncs with identical orientations. Such a coalescence process is similar to that observed by Wang et al. [20] for silicon nanocrystals (Si-ncs). It can be explained by energy minimization effects at the boundary of primary nanograins. Since the {111} planes are the faces with the lower energy in the cubic closed-packed Ge crystal, the coalescence of several particles through {111}

Table 1 – Average sizes and spatial distributions of Ge ncs at different annealing temperatures.

Annealing temperature (°C)	Average size (nm)	Implanted layer thickness (nm)
700	5.95	70
800	6.13	70
850	6.33	62
900	10.31	65
1000	15.49	65
1100	28.15	60

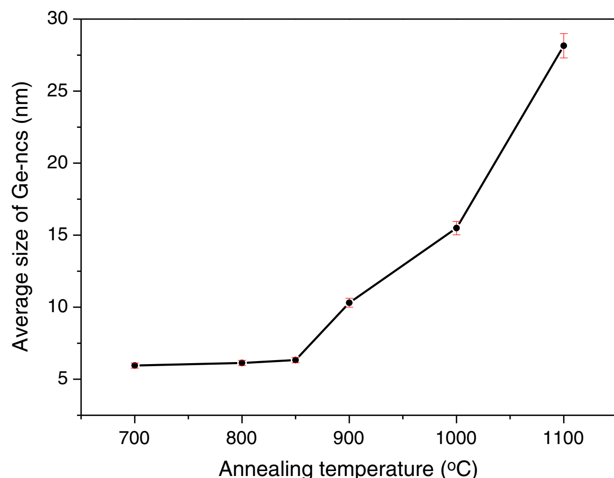

Fig. 3 – The relationship between the average size of Ge-ncs and the annealing temperatures.

planes is energetically favorable. Besides the nanocrystals with twinning defects, nanocrystals without defects are also frequently observed. In Fig. 5(c), the high crystallinity of observed Ge-ncs may be related to their small size (<6 nm), as previously reported for silicon nanocrystals smaller than 5 nm [21]. This can result from greater elastic deformation inside small nanoparticles, where the high surface to volume ratio can favor the energy release, as well as the gliding of dislocations towards the Ge-nc boundaries. Fig. 5(d) shows a typical SAED pattern of Ge-ncs embedded in amorphous SiO_2. From the diffraction pattern, using the lattice parameter of bulk Ge (a = 5.658 Å), three diffraction rings are clearly identified as the {111}, {220} and {311}, respectively. It can also be seen from Fig. 5(d) that the crystal structures of Ge-ncs do not have any preferential orientation.

For samples annealed at 800 °C, apart from the above-mentioned twinning defects, five-fold twins and dislocations start to show up in some nanocrystals, as observed in Fig. 6(a). Both the dislocation and the five-fold twin are enlarged in Fig. 6(b). The twin planes observed in nanocrystal C are {111} planes and the twin boundaries are indicated by white arrows, labeled with TB1, TB2 and TB3, respectively. In Fig. 6(b), we find that the five-fold twin is composed of five variants at the interface between the nanoparticles B and C. We think that this five-fold twin results from the coalescence of several small nanocrystals with different structural orientations, during the annealing. The angles measured from the adjacent twin boundaries are: 1) 67.7°, 2) 81.6°, 3) 71.1°, 4) 71.8° and 5) 67.8°. The discrepancy of these five angles may result from a residual local stress. The angle between two adjacent {111} twin variants in equilibrium should be 70.53° in a cubic structure, thus leading to a solid-angle deficiency of 7.35° for the five-fold twin observed in Fig. 6(b). Consequently, such nanoparticles should contain defects or be intrinsically strained [22]. This suggests that some Ge-ncs may have an excess of internal energy that aims to be released through the formation of defects [23]. For example, an edge dislocation is observed close to the five-fold twinning, labeled with D and indicated by dashed lines in Fig. 6(b).

Table 2 – Statistical results of defects at different annealing temperatures.

Temperature (°C)	Planar defect percent (%)		Dislocation percent (%)	Perfect (%)
	Twinning defect	Stacking fault		
700	35.48	46.77	8.07	9.68
800	44.69	26.25	16.56	12.50
850	39.06	26.56	18.75	15.63
900	35.00	29.00	26.00	10.00
1000	37.50	29.17	20.83	12.50
1100	23.79	20.21	34.57	21.43

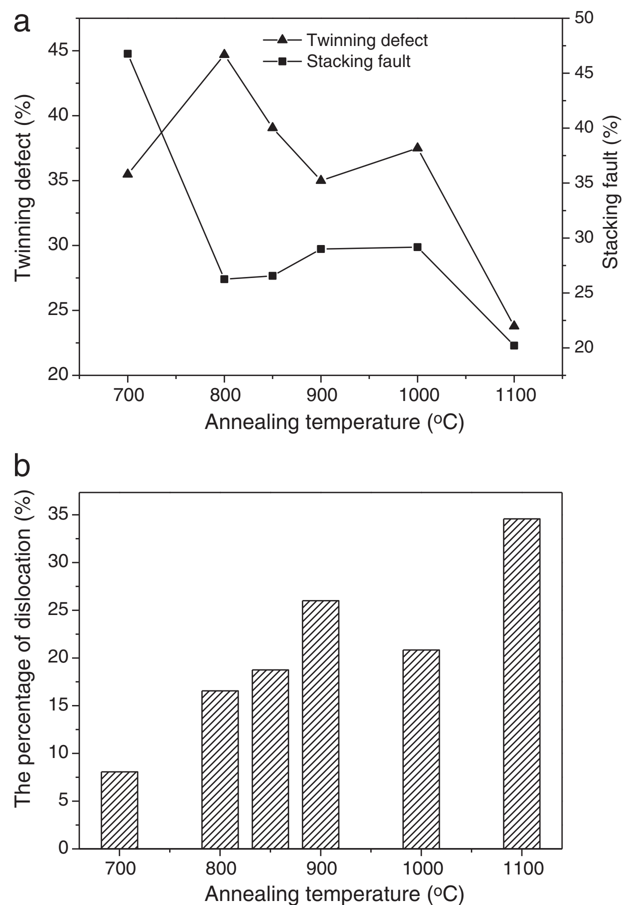

Fig. 4 – (a) The changing trend of planar defects (i.e. twinning defects and stacking faults) with annealing temperature; (b) the changing trend of dislocation with annealing temperature.

Fig. 7 shows typical HRTEM images of the sample annealed at 850 °C. Although the twinning defects are still dominant in nanoparticles synthesized at this temperature, a great number of dislocations are detected. An example of Ge-ncs with twins is illustrated in Fig. 7(a). In addition, nanoparticles with different crystal orientations that are about to combine together are shown in Fig. 7(b). Careful examination indicates that a dislocation exists near the boundary of a nanotwin in the lower-left corner, which is similar to that shown in Fig. 6(b). In some specific regions of large nanoparticles, we also observed several dislocations, as shown in Fig. 7(c), where three dislocations are detected close to the interface of nanocrystals A and B.

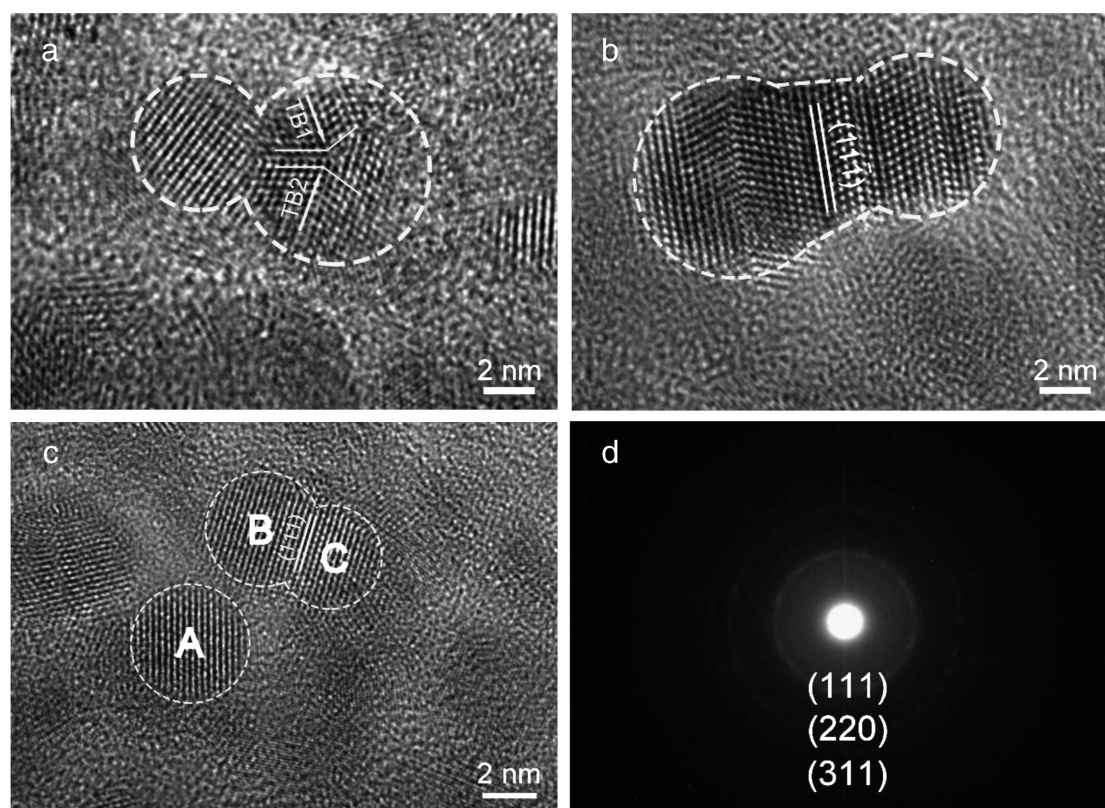

Fig. 5 – Typical HRTEM images of the sample annealed at 700 °C. (a) Two particles about to combine together, the bigger one composed of two twins with different orientation combining together; (b) three particles with a twinning structure about to combine together in appropriate orientation (the combination of three particles with a twinning structure); (c) an individual Ge nanocrystal A and a coalesced nanocrystal composed of particle B and C; (d) typical SAED pattern from Ge ncs in this sample.

These dislocations are aligned to the boundary of these two coalesced nanoparticles. We believe that in addition to relaxing the local stress, the formation of successive dislocations similar to those shown in Fig. 6(c) can promote the ordering of crystal planes during the coalescence process.

When the annealing temperature reaches 900 °C, a significant increase of both the nanocrystal size and the dislocation concentration are observed. As shown in Fig. 8 the size of the observed nanoparticle is about 10 nm. Such an increase of the Ge-nc dimensions may result from the clustering of many small Ge-ncs with different crystal orientations during the annealing. Careful examination of Fig. 8 shows that there are two perfect dislocations and one extended dislocation. The two perfect dislocations are indicated by D1 and D2. It is clear that the Burgers vectors for D1 and D2 have opposite signs, indicating that these two dislocations attract each other. If such antiparallel dislocations meet, they will generally recombine and annihilate. Here D1 and D2 do not lie on the same gliding plane, so that these two dislocations have an equilibrium configuration where they do not completely compensate each other. As for the existence of extended dislocation, it can be interpreted from an energy point of view that the dissociation of one perfect dislocation into two partial ones is more energetically favorable [24]. Consequently, in addition to size effects, the high percentage of dislocations observed in Ge-ncs prepared at 900 °C seems to be compatible with the dissipation of a greater energy during their synthesis [15].

When the annealing is performed at 1000 °C, which is higher than the Ge melting point of 937 °C, the percentage of observed dislocations decreases surprisingly, while the average size of synthesized Ge-ncs increases significantly. As shown in Fig. 9, the lattices of some Ge-ncs are nearly perfect. Only a low percentage of defects are detected in all observed nanocrystals. Fig. 9(a) shows a twinning defect in the upper-right corner of the nanocrystal, zoomed in Fig. 9(b). In addition, there is a dislocation in the centre of the nanocrystal shown in Fig. 9(c), zoomed in Fig. 9(d).

For Ge-ncs prepared at 1100 °C, the percentage of dislocations increases significantly with respect to that of the sample annealed at 1000 °C. Fig. 10 shows two examples of Ge-ncs annealed at 1100 °C. Their dimensions are measured to be 27 nm and 30 nm from Fig. 10(a) and (b), respectively. From the second column of Table 1, it can be seen that the average size of Ge-ncs synthesized at 1100 °C is almost twice as large as those prepared at 1000 °C. Most Ge-ncs observed in the sample annealed at 1100 °C are composed of several nanocrystals. Two dislocations are detected in Fig. 10(a), whereas stacking faults and dislocations are both observed in Fig. 10(b).

The interplanar distances of Ge-ncs synthesized at 700 °C, 800 °C, 850 °C, 900 °C, 1000 °C and 1100 °C were measured from the HRTEM images of Ge-ncs. These values are given in the second column of Table 3. They allow us to estimate the residual stress to which each spacing variation corresponds, as reported in the third column of Table 3, where the relative

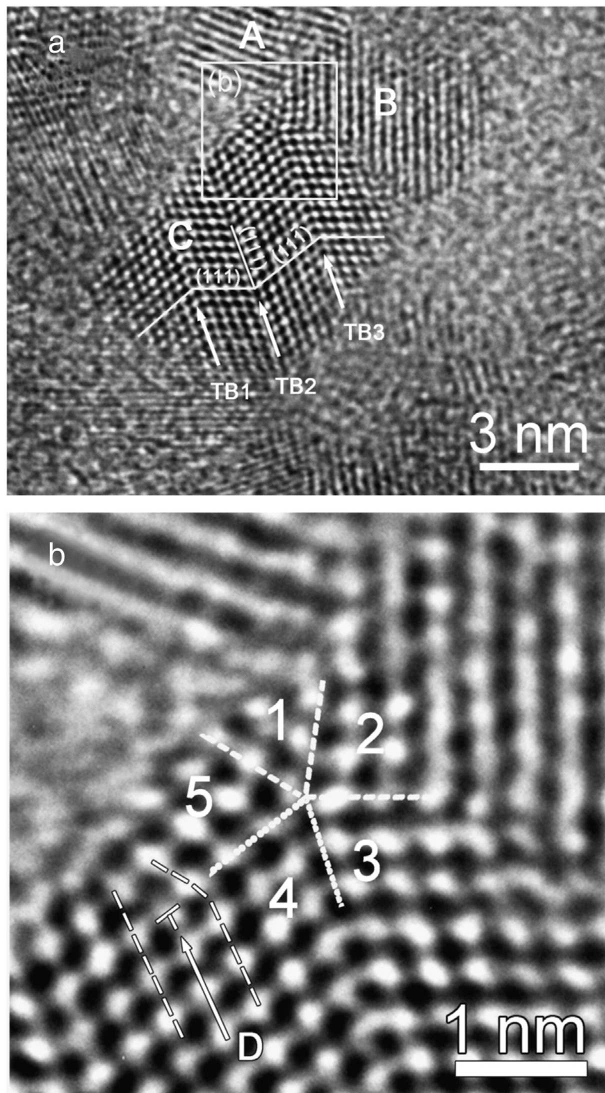

Fig. 6 – Typical HRTEM images of defects observed in the sample annealed at 800 °C. (a) Typical HRTEM image showing the combination of three nanocrystals; (b) an enlarged HRTEM image of the region enclosed by a rectangle in Fig. 5(a), where five-fold twin and dislocation are found.

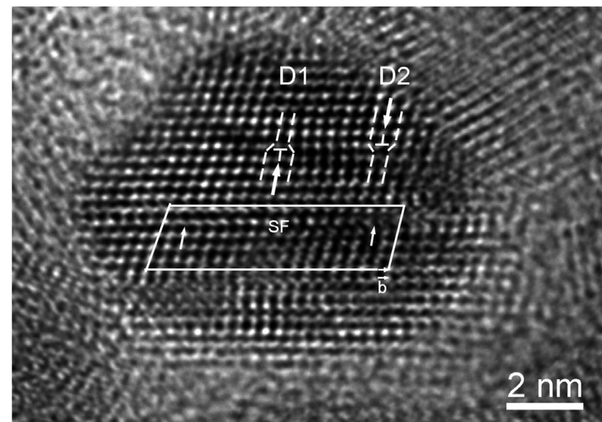

Fig. 8 – Typical HRTEM image of a nanoparticle containing two perfect dislocations with Burgers vectors of opposite signs and an extended dislocation formed after annealing at 900 °C.

compressive stress of 4.3% obtained from Ge-ncs prepared at 1100 °C is very close to the stress measured by Choi et al. using the Raman spectroscopy technique [25]. In Fig. 11(a), it is clear that the change of the residual stress is consistent with the variation of the interplanar spacing at different annealing temperatures. In Fig. 11(b), the values of the relative residual stress extracted from our TEM observation are compared with the dislocation concentrations reported in Table 2. As clearly evidenced on Fig. 11(b), the evolution of the residual stress inside Ge-ncs follows the same trend as that of the dislocation concentration. Namely, it gradually increases from 700 °C to 900 °C, decreases between 900 °C and 1000 °C, and then drastically increases from 1000 °C to 1100 °C. Such a remarkable feature demonstrates that the observed dislocations are strongly correlated with the residual stress field inside Ge-ncs. Hence, the formation of such defects provides a good way for the Ge-ncs to release the energy accumulated during their nucleation.

According to our results, we can propose the following scenarios for explaining the evolution of microstructural defect in the Ge-ncs. Three different growth regimes can be differentiated for thermal annealing performed at a temperature below, close to and above the melting point of bulk Ge, respectively. Between 700 °C and 900 °C, both planar and linear defects are

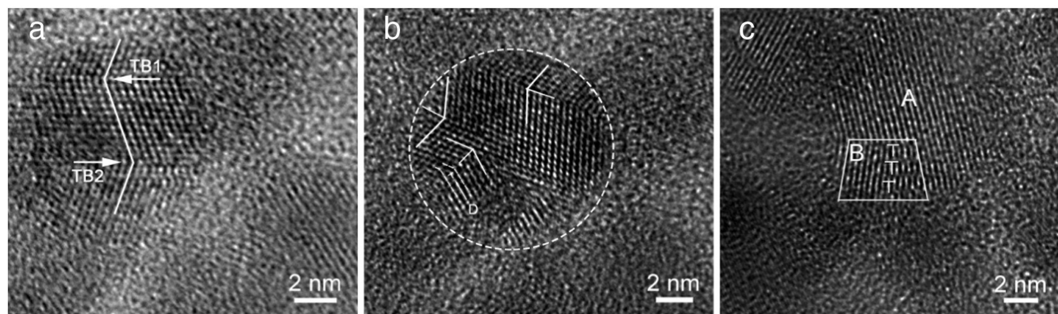

Fig. 7 – HRTEM images of the sample annealed at 850 °C. (a) [011] zone-axis HRTEM image of a single Ge nanoparticle with nanotwins; (b) twins with different orientations about to combine together and a dislocation observed at the twin boundary of the nanoparticle at the lower-left corner; (c) nanocrystals with different orientations combined together with dislocations that occurred in the interface between nanocrystals A and B.

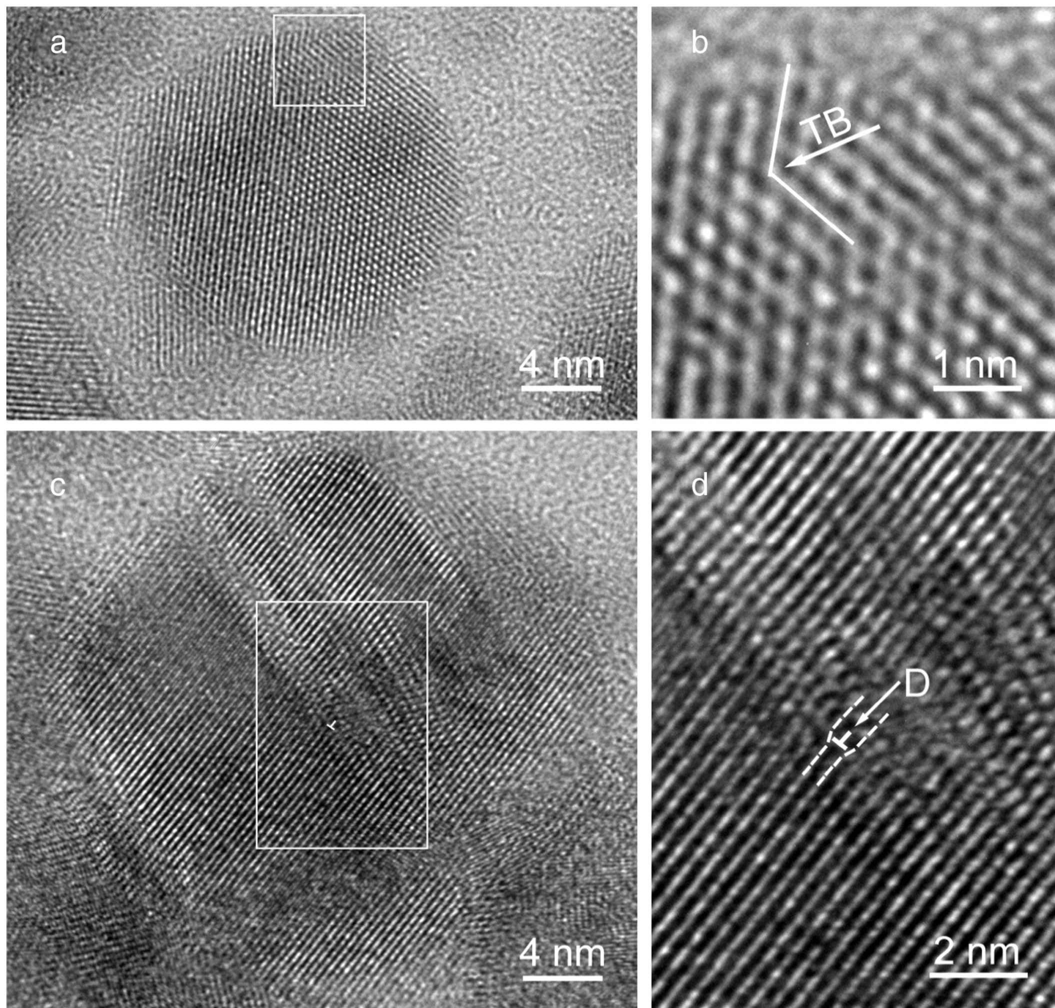

Fig. 9 – HRTEM images of the sample annealed at 1000 °C. (a) Particle with twining defect in the top-right corner; (b) an enlarged HRTEM corresponding to the region enclosed by a rectangle in (a); (c) nanoparticle with dislocation; (d) magnified image from the rectangle enclosed area in (c).

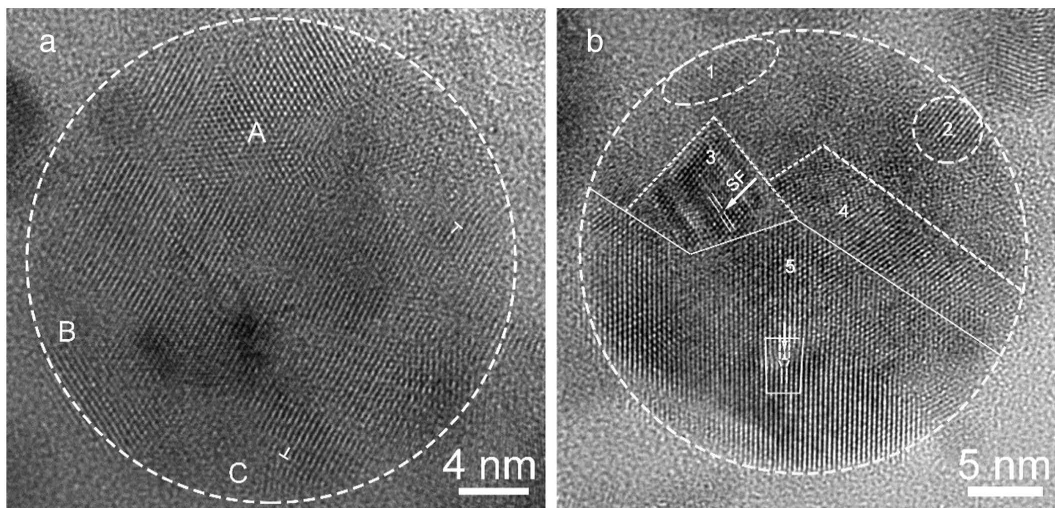

Fig. 10 – Typical HRTEM images of nanocrystals annealed at 1100 °C. (a) A nanoparticle composed of three crystals, in which two dislocations were observed; (b) a nanoparticle composed of five crystals with different orientations, in which stacking fault and dislocation were observed in this particle.

Table 3 – Interplanar spacings of Ge-ncs at different annealing temperatures, with relative compressive stress calculated with respect to the interplanar distance of bulk Ge.

Annealing temperature (°C)	Interplanar spacing (nm)	Residual stress (%)
700	0.3214	1.6
800	0.3193	2.3
850	0.3180	2.7
900	0.3177	2.8
1000	0.3200	2.1
1100	0.3125	4.3

mainly associated with the coalescence of small nanoparticles, whose occurrence frequency increases with annealing temperature. Some twinning structures observed in these Ge-ncs can be regarded as a result of the coalescence of two (or more) Ge-ncs, as already reported for silicon nanocrystals [21]. During the coalescence process, Ge atoms tend to reorganize and align their crystal planes [26], thus leading to the formation of an increasing number of dislocations that can reduce the excessive stress in the system. But due to some limitations in this re-ordering process, only a fraction of the Ge-ncs internal stress is dissipated, so that a local stress field can still remain at the interface of small coalesced Ge-ncs and/or in the vicinity of the structural defects. Such a description of the Ge-ncs

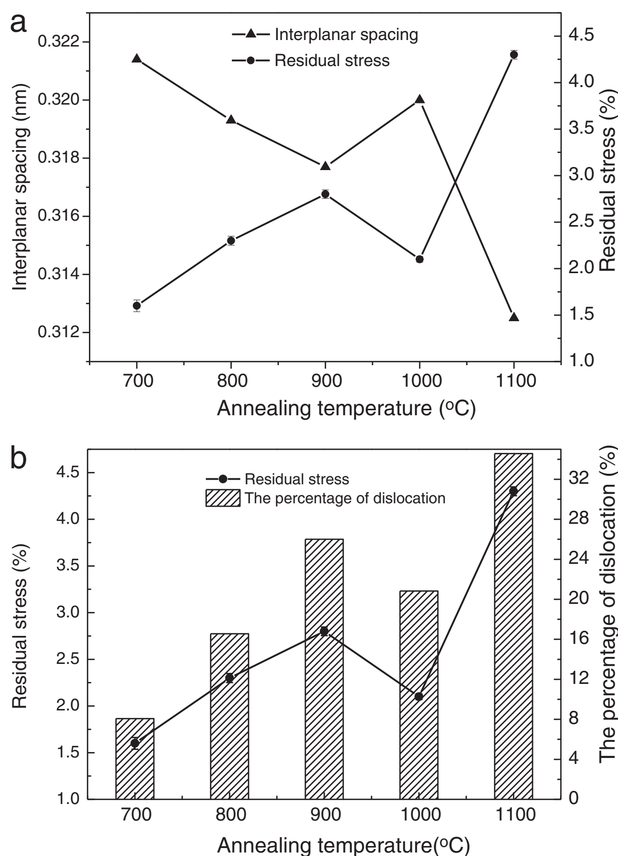

Fig. 11 – (a) The changes of interplanar spacing and residual stress with annealing temperature as reported in Table 3; (b) comparison between the relative concentration of dislocations and the residual stress intensity.

growth between 700 °C and 900 °C is strongly corroborated by the continuous increase of the Ge-nc size, along with that of both the dislocation concentration and the residual stress inside the formed Ge-ncs. At 1000 °C, namely for an annealing temperature slightly above the solid–liquid transition of Ge, small Ge nanodroplets coalesce into larger nanodroplets, where the melting of Ge-ncs improves the diffusion of Ge atoms. All stress effects related to the clustering of Ge atoms coming from nanoparticles with different crystal orientations become negligible, as well as the energy accumulation caused by reordering effects. During the cooling of samples annealed at 1000 °C, the liquid–solid transition of Ge nanodroplets into Ge nanocrystallites may be sufficiently smooth to minimize the heterogeneous nucleation effects reported by Xu et al. [27], which can generate plenty of structural defects. However, the decrease of the Ge atom density at the liquid–solid phase transition enhances the volume of the formed Ge nanoclusters. This generates a compressive stress at the Ge-ncs/silica interface which is partially relaxed by the formation of dislocations during the sample cooling. For Ge-ncs prepared at 1100 °C, both the volume expansion effects and the sample cooling velocity are enhanced, as a result of the drastic increase of the Ge nanocluster dimensions and the higher temperature of thermal annealing, respectively. In addition to the effect on the kinetics of Ge-nc nucleation, these features could also increase the formation of structural defects associated with volume expansion of about 6%, which are exerted by the surrounding SiO_2 matrix on Ge-ncs during the sample cooling [25,28]. We also suspect that the greater thermal instability of large aggregates reduces the Ge atom ordering inside Ge-ncs.

4. Conclusions

In summary, Ge-ncs synthesized at annealing temperatures varying from 700 °C to 1100 °C has been investigated by TEM experiments. The image analysis indicates that the size of Ge-ncs increases with the annealing temperature. HRTEM micrographs show the presence of linear and planar defects, especially dislocations, twinning defects and stacking faults. By comparing the annealing temperature-dependence of the dislocation concentration with the residual compressive stress measured inside Ge-ncs, we have evidenced a strong correlation between the formation of defects and the stress field relaxation. A description of the mechanisms involved in the nucleation of Ge-ncs is proposed for each Ge-nc growing regime, below, around and above the melting point of bulk Ge. This work provides qualitative fundamental insight regarding both the presence of microstructural defects and the origin of the residual stress field within Ge-ncs. It also gives crucial information for designing Ge-ncs of high crystallinity with suitable dimensions, for the development of new advanced materials.

Acknowledgments

The work is financially supported by the National Key Basic Research Development Program of China (Grant no.: 2012CB722705), the Natural Science Foundation for Outstanding Young Scientists in Shandong Province, China (Grant no.:

JQ201002), and the Program for Foreign Cultural and Educational Experts (Grant nos.: W20123702084, W20133702021, GDW20123702162). Y. Q. Wang thanks the financial support from the Top-notch Innovative Talent Program of Qingdao City and the Taishan Scholar Program of Shandong Province, China.

REFERENCES

[1] Nguyen PD, Kepaptsoglou DM, Erni R, Ramasse QM, Olsen A. Phys Rev B 2012;86:245316.
[2] Barba D, Martin F, Demarche J, Terwagne G, Ross GG. Nanotechnology 2012;23:145701.
[3] Kanemitsu Y, Uto H, Masumoto Y, Maeda Y. Appl Phys Lett 1992;61:2187.
[4] Maeda Y, Tsukamoto N, Yazawa Y, Kanemitsu Y, Masumoto Y. Appl Phys Lett 1991;59:3168.
[5] Bregolin FL, Behar M, Sias US, Moreira EC. Nucl Inst Methods Phys Res B 2009;267:1321–3.
[6] Rebohle L, von Borany J, Yankov RA, Skorupa W, Tyschenko IE, Fröb H, et al. Appl Phys Lett 1997;71:2809.
[7] Kamata Y. Mater Today 2008;11:30–8.
[8] Nozik AJ. Nat Photonics 2012;6:272–3.
[9] Serincan U, Yerci S, Kulakci M, Turan R. Nucl Inst Methods Phys Res B 2005;239:419–25.
[10] Zhu JG, White CW, Budai JD, Withrow SP, Chen Y. J Appl Phys 1995;78:4386.
[11] Desnica UV, Dubcek P, Salamon K, Desnica-Frankovic ID, Buljan M, Bernstorff S, et al. Nucl Inst Methods Phys Res B 2005;238:272–5.
[12] Yamamoto M, Koshikawa T, Yasue T, Harima H, Kajiyama K. Thin Solid Films 2000;369:100–3.
[13] Beyer R, Borany J. Surf Interface Anal 2012;44:1018–21.
[14] Marstein E, Gunnæs A, Serincan U, Turan R, Olsen A, Finstad T. Surf Coat Technol 2002;158:544–7.
[15] Rudolph P. In: Dhanaraj G, Byrappa K, et al, editors. Springer handbook of crystal growth. Berlin: Springer; 2010. p. 159–201.
[16] Biersack J, Haggmark L. Nucl Instrum Meth 1980;174:257–69.
[17] Wu XL, Gao T, Bao XM, Yan F, Jiang SS, Feng D. J Appl Phys 1997;82:2704.
[18] Gryaznov V, Polonsky I, Romanov A, Trusov L. Phys Rev B 1991;44:42–6.
[19] Narayan J. J Appl Phys 2006;100:034309.
[20] Wang Y, Smirani R, Ross GG, Schiettekatte F. Phys Rev B 2005;71:161310R.
[21] Wang Y, Smirani R, Ross GG. Nano Lett 2004;4:2041–5.
[22] Mayoral A, Barron H, Estrada-Salas R, Vazquez-Duran A, Jose-Yacaman M. Nanoscale 2010;2:335–42.
[23] Ding YH, Cai RS, Wang YQ, Chen YZ, Sun JR. Mater Lett 2012;67:67–9.
[24] Ding Y, Sun XL, Wang ZL, Sun SL. Appl Phys Lett 2012;100:111603.
[25] Choi WK, Chew HG, Zheng F, Chim WK, Foo YL, Fitzgerald EA. Appl Phys Lett 2006;89:113126.
[26] Jose-Yacaman M, Gutierrez-Wing C, Miki M, Yang D-Q, Piyakis K, Sacher E. J Phys Chem B 2005;109:9703–11.
[27] Xu Q, Sharp I, Yuan C, Yi D, Liao C, Glaeser A, et al. Phys Rev Lett 2006;97:155701.
[28] Wellner A, Paillard V, Bonafos C, Coffin H, Claverie A, Schmidt B, et al. J Appl Phys 2003;94:5639.